A Six-Phase Series-Connected Two-Motor Drive With Decoupled Dynamic Control

Martin Jones, Slobodan N. Vukosavic, *Member, IEEE*, Emil Levi, *Senior Member, IEEE*, and Atif Iqbal

***Abstract*—This paper analyzes a six-phase two-motor drive, consisting of a six-phase voltage-source inverter (VSI), a six-phase induction machine, and a three-phase induction machine. Stator windings of the two machines are connected in series in an appropriate manner. This enables full decoupling of the dynamics of the two machines by means of vector control. Detailed mathematical modeling of the system is performed and the set of *d–q* equations, describing the two machines connected in series to a six-phase VSI, is developed. The resulting model clearly shows the possibility of independent vector control of the two machines, although a single VSI is used as the supply. An experimental rig is constructed and existence of the decoupled dynamic control of the two machines supplied from a single VSI is fully verified by extensive experimental testing.**

***Index Terms*—Multimotor drives, multiphase machines, six-phase, vector control.**

I. Introduction

SIX-PHASE ac motor drives are often considered as viable solutions when reduction of the inverter per-phase rating is required due to the high motor power. Although the basic concept is old [1], there has been an upsurge in the interest in this type of ac motor drive in recent time [2]–[5]. The standard choice is a six-phase induction or synchronous machine with two three-phase windings on the stator. The spatial displacement between the two three-phase windings is 30° (so-called quasi-six-phase machine) and neutral points of the two windings can be isolated or connected. The main reason for selecting the asymmetrical six-phase winding instead of the true six-phase winding (60° displacement between any two consecutive phases), elimination of the sixth harmonic from the torque [1], was important in the pre-pulsewidth-modulation (PWM) era of voltage-source inverter (VSI) control. It is nowadays less relevant since good inverter current control in PWM mode can eliminate low-order harmonics from the inverter output currents. A true six-phase induction motor is used in the work described here, with the underlying idea of realizing a two-motor drive system with independent vector control, while utilizing a single six-phase VSI as the supply.

The two-motor drive system is realized by connecting in series with such a six-phase induction machine, the second, three-phase induction machine. The appropriate series connection of the stator windings of the two machines should enable, according to [6], independent and decoupled vector control of the two machines, although a single six-phase inverter supply is used. The six-phase series-connected two-motor drive is one particular case of a much wider concept, which is applicable to any phase number greater than or equal to five. It relies on the fact that any n-phase ac machine, regardless of the type, requires only two currents for independent flux and torque control [6], [7]. A general study for all the possible even phase numbers has been reported in [6] while a corresponding study for odd phase numbers can be found in [7]. Studies reported in [6] and [7] were based on physical and intuitive reasoning and they provide verification of the concept by simulation. Detailed mathematical models of series-connected multiphase multimotor drive systems of [6], [7] do not exist at present, except for the two-motor five-phase drive [8]. Moreover, the concept has never been proved before by experimental investigation for any phase number.

The purpose of this paper is twofold. In the first part of the paper (Sections II–IV), a rigorous mathematical modeling of the six-phase series-connected two-motor drive system is reported. The final result is a model in the rotor flux oriented reference frames of the two machines. This model confirms mathematically the existence of means for independent rotor flux oriented control of the two-motor drive system. The second part of the paper (Sections V and VI) at first describes the experimental rig, constructed with the aim of verifying the existence of the completely decoupled dynamic control of the two machines. This is followed by presentation of results collected from the rig for relevant transients (acceleration, deceleration, reversing, and step loading/unloading). The complete decoupling of the dynamics of the two machines is thus confirmed experimentally. Conclusions are drawn in VII

The six-phase series-connected two-motor drive is seen as well suited for applications where a six-phase motor drive is used anyway due to high power requirements. In many such situations there is a need for an auxiliary low-power motor drive, which has to be controlled independently. In such cases proposed series connection enables control of the second machine at no extra cost, since the existing inverter can be utilized. One possible application of this type is in locomotive traction, where high-power six-phase machines are already utilized as main driving motors. The two-motor arrangement of this paper

Paper IPCSD-05-028, presented at the 2004 Industry Applications Society Annual Meeting, Seattle, WA, October 3–7, and approved for publication in the IEEE Transactions on Industry Applications by the Industrial Drives Committee of the IEEE Industry Applications Society. Manuscript submitted for review July 8, 2004 and released for publication April 6, 2005. This work was supported by the Engineering and Physical Sciences Research Council under Standard Research Grant GR/R64452/01 and by Semikron Ltd. The work of M. Jones was also supported by the Institution of Electrical Engineers, U.K. (IEE), through the IEE Robinson Research Scholarship.

The authors are with the School of Engineering, Liverpool John Moores University, Liverpool, L3 3AF, U.K. (e-mail: m.jones2@livjm.ac.uk; boban@ieee.org; e.levi@livjm.ac.uk; atif_iqbal1@rediffmail.com).

Digital Object Identifier 10.1109/TIA.2005.851020

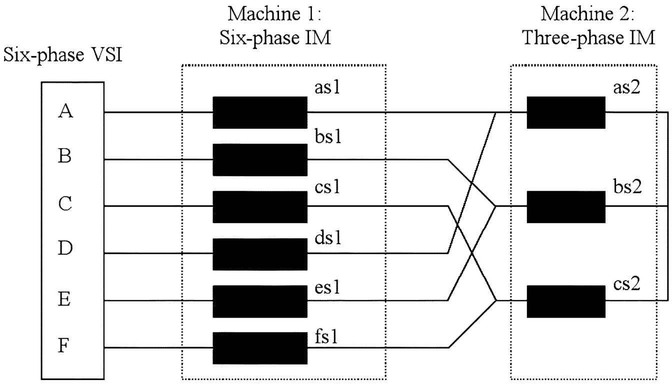

Fig. 1. Six-phase series-connected two-motor drive system.

enables connection of the second (three-phase) machine with utilization of the existing inverter. The second motor drive could be used for cooling and/or ventilation.

II. Configuration of the Two-Motor Drive

The two-motor drive, analyzed in the paper, is shown in Fig. 1. It consists of a six-phase VSI (capital letters A, B, ... F), a six-phase, and a three-phase ac machine. Stator windings of the two machines are connected in series (Fig. 1). The six-phase machine has the spatial displacement between any two consecutive stator phases of 60° (i.e., $\alpha = 2\pi/6$). As already noted, the type of the ac machine is irrelevant as long as the magnetomotive force (MMF) distribution in the air gap is sinusoidal. Both machines are for the modeling and experimentation purposes taken here as induction motors. Spatial displacement between any two consecutive phases of the three-phase machine is $2\alpha = 120°$.

Inverter phase-to-neutral voltages are related to individual machine phase voltages through (Fig. 1)

$$\underline{v}^{\mathrm{INV}} = \begin{bmatrix} v_A \\ v_B \\ v_C \\ v_D \\ v_E \\ v_F \end{bmatrix} = \begin{bmatrix} v_{as1} + v_{as2} \\ v_{bs1} + v_{bs2} \\ v_{cs1} + v_{cs2} \\ v_{ds1} + v_{as2} \\ v_{es1} + v_{bs2} \\ v_{fs1} + v_{cs2} \end{bmatrix} \tag{1}$$

where indexes 1 and 2 identify the two machines in Fig. 1 and index s stands for stator. Relationship between source currents and individual stator phase currents of the two motors is governed with (Fig. 1)

$$\underline{i}_{s1} = \begin{bmatrix} i_{as1} \\ i_{bs1} \\ i_{cs1} \\ i_{ds1} \\ i_{es1} \\ i_{fs1} \end{bmatrix} = \begin{bmatrix} i_A \\ i_B \\ i_C \\ i_D \\ i_E \\ i_F \end{bmatrix} = \underline{i}^{\mathrm{INV}}$$
$$\underline{i}_{s2} = \begin{bmatrix} i_{as2} \\ i_{bs2} \\ i_{cs2} \end{bmatrix} = \begin{bmatrix} i_A + i_D \\ i_B + i_E \\ i_C + i_F \end{bmatrix}. \tag{2}$$

It is assumed that the standard modeling assumptions apply, including the one related to the sinusoidal distribution of the field in the machine. Rotor winding of the six-phase machine is taken as six-phase as well, for the sake of generality.

III. Modeling of the Two-Motor Drive

A. Phase-Variable Model

The electrical subsystem's model of the drive in Fig. 1 is of the 15th order. It can be given in matrix form with

$$\underline{v} = \underline{R}\underline{i} + \frac{d(\underline{L}\underline{i})}{dt} \tag{3}$$

where

$$\underline{v} = [\underline{v}^{\mathrm{INV}} \quad \underline{0} \quad \underline{0}]^T \quad \underline{i} = [\underline{i}^{\mathrm{INV}} \quad \underline{i}_{r1} \quad \underline{i}_{r2}]^T. \tag{4}$$

Rotor current vector matrices of (4) are

$$\underline{i}_{r1} = [i_{ar1} \quad i_{br1} \quad i_{cr1} \quad i_{dr1} \quad i_{er1} \quad i_{fr1}]^T \tag{5a}$$
$$\underline{i}_{r2} = [i_{ar2} \quad i_{br2} \quad i_{cr2}]^T. \tag{5b}$$

Matrix (3) can be given as

$$\begin{bmatrix} \underline{v}^{\mathrm{INV}} \\ \underline{0} \\ \underline{0} \end{bmatrix} = \begin{bmatrix} \underline{R}_{s1} + \underline{R}'_{s2} & & \\ & \underline{R}_{r1} & \\ & & \underline{R}_{r2} \end{bmatrix} \begin{bmatrix} \underline{i}^{\mathrm{INV}} \\ \underline{i}_{r1} \\ \underline{i}_{r2} \end{bmatrix} + \frac{d}{dt}\left\{ \begin{bmatrix} \underline{L}_{s1} + \underline{L}'_{s2} & \underline{L}_{sr1} & \underline{L}'_{sr2} \\ \underline{L}_{rs1} & \underline{L}_{r1} & \underline{0} \\ \underline{L}'_{rs2} & \underline{0} & \underline{L}_{r2} \end{bmatrix} \begin{bmatrix} \underline{i}^{\mathrm{INV}} \\ \underline{i}_{r1} \\ \underline{i}_{r2} \end{bmatrix} \right\}. \tag{6}$$

Primed symbol $'$ in (6) denotes submatrices that have been modified through the series connection of Fig. 1, when compared to the form they take for a single three-phase motor drive. These submatrices are determined with

$$\underline{R}'_{s2} = \begin{bmatrix} \underline{R}_{s2} & \underline{R}_{s2} \\ \underline{R}_{s2} & \underline{R}_{s2} \end{bmatrix}$$
$$\underline{L}'_{s2} = \begin{bmatrix} \underline{L}_{s2} & \underline{L}_{s2} \\ \underline{L}_{s2} & \underline{L}_{s2} \end{bmatrix} \tag{7}$$
$$\underline{L}'_{sr2} = \begin{bmatrix} \underline{L}_{sr2} \\ \underline{L}_{sr2} \end{bmatrix}$$
$$\underline{L}'_{rs2} = [\underline{L}_{rs2} \quad \underline{L}_{rs2}] = [\underline{L}^T_{sr2} \quad \underline{L}^T_{sr2}]. \tag{8}$$

The resistance and inductance submatrices without the prime symbol have the usual meaning. Torque equations of the two machines, in terms of source currents, are shown by (9) and (10), at the bottom of the next page.

B. Application of the Decoupling Transformation

Let the correlation between original phase variables and new variables be given with $\underline{f}_{\alpha\beta} = \underline{C}_{(6)}\underline{f}_{abcdef}$, where $\underline{C}_{(6)}$ is the power-invariant transformation matrix (11), shown at the bottom of the page. The corresponding matrix for the three-phase system is

$$\underline{C}_{(3)} = \sqrt{\frac{2}{3}}\begin{array}{c}\alpha\\ \beta\\ 0\end{array}\left|\left[\begin{array}{ccc}1 & \cos 2\alpha & \cos 4\alpha\\ 0 & \sin 2\alpha & \sin 4\alpha\\ 1/\sqrt{2} & 1/\sqrt{2} & 1/\sqrt{2}\end{array}\right]\right. . \tag{12}$$

Application of the transformation matrix (11) in conjunction with the first two rows of (6) and application of (12) in conjunction with the third row of (6) lead to the decoupled model of the six-phase two-motor drive system. Rotor voltage equations of the six-phase machine become

$$\begin{aligned}
0 &= R_{r1} i_{\alpha r1} + L_{r1}\frac{di_{\alpha r1}}{dt}\\
&\quad + \frac{d}{dt}L_{m1}\left(\cos\theta_1 i_\alpha^{\mathrm{INV}} + \sin\theta_1 i_\beta^{\mathrm{INV}}\right)\\
0 &= R_{r1} i_{\beta r1} + L_{r1}\frac{di_{\beta r1}}{dt}\\
&\quad + \frac{d}{dt}L_{m1}\left(-\sin\theta_1 i_\alpha^{\mathrm{INV}} + \cos\theta_1 i_\beta^{\mathrm{INV}}\right)\\
0 &= R_{r1} i_k + L_{lr1}\frac{di_k}{dt}, \qquad k = xr1, yr1, 0+r1, 0-r1.
\end{aligned} \tag{13}$$

Similarly, for the rotor of the three-phase machine one obtains

$$\begin{aligned}
0 &= R_{r2} i_{\alpha r2} + L_{r2}\frac{di_{\alpha r2}}{dt}\\
&\quad + \frac{d}{dt}\sqrt{2}L_{m2}\left(\cos\theta_2 i_x^{\mathrm{INV}} + \sin\theta_2 i_y^{\mathrm{INV}}\right)\\
0 &= R_{r2} i_{\beta r2} + L_{r2}\frac{di_{\beta r2}}{dt}\\
&\quad + \frac{d}{dt}\sqrt{2}L_{m2}\left(-\sin\theta_2 i_x^{\mathrm{INV}} + \cos\theta_2 i_y^{\mathrm{INV}}\right)\\
0 &= R_{r2} i_{0r2} + L_{lr2}\frac{di_{0r2}}{dt}.
\end{aligned} \tag{14}$$

Source voltage equations, which include equations of the two stator windings connected in series, can be given as

$$\begin{aligned}
v_\alpha^{\mathrm{INV}} &= R_{s1} i_\alpha^{\mathrm{INV}} + L_{s1}\frac{di_\alpha^{\mathrm{INV}}}{dt}\\
&\quad + L_{m1}\frac{d}{dt}(\cos\theta_1 i_{\alpha r1} - \sin\theta_1 i_{\beta r1})\\
v_\beta^{\mathrm{INV}} &= R_{s1} i_\beta^{\mathrm{INV}} + L_{s1}\frac{di_\beta^{\mathrm{INV}}}{dt}\\
&\quad + L_{m1}\frac{d}{dt}(\sin\theta_1 i_{\alpha r1} + \cos\theta_1 i_{\beta r1})\\
v_x^{\mathrm{INV}} &= R_{s1} i_x^{\mathrm{INV}} + L_{ls1}\frac{di_x^{\mathrm{INV}}}{dt}\\
&\quad + \sqrt{2}\left(\begin{array}{l} R_{s2}\sqrt{2}i_x^{\mathrm{INV}} + L_{s2}\frac{d\sqrt{2}i_x^{\mathrm{INV}}}{dt}\\ +L_{m2}\frac{d}{dt}(\cos\theta_2 i_{\alpha r2} - \sin\theta_2 i_{\beta r2})\end{array}\right)\\
v_y^{\mathrm{INV}} &= R_{s1} i_y^{\mathrm{INV}} + L_{ls1}\frac{di_y^{\mathrm{INV}}}{dt}\\
&\quad + \sqrt{2}\left(\begin{array}{l} R_{s2}\sqrt{2}i_y^{\mathrm{INV}} + L_{s2}\frac{d\sqrt{2}i_y^{\mathrm{INV}}}{dt}\\ +L_{m2}\frac{d}{dt}(\sin\theta_2 i_{\alpha r2} + \cos\theta_2 i_{\beta r2})\end{array}\right)\\
v_{0+}^{\mathrm{INV}} &= R_{s1} i_{0+}^{\mathrm{INV}} + L_{ls1}\frac{di_{0+}^{\mathrm{INV}}}{dt}\\
&\quad + \sqrt{2}\left(R_{s2}\sqrt{2}i_{0+}^{\mathrm{INV}} + L_{ls2}\frac{d\sqrt{2}i_{0+}^{\mathrm{INV}}}{dt}\right)\\
v_{0-}^{\mathrm{INV}} &= R_{s1} i_{0-}^{\mathrm{INV}} + L_{ls1}\frac{di_{0-}^{\mathrm{INV}}}{dt}.
\end{aligned} \tag{15}$$

Magnetizing inductances in (13)–(15) are $L_{m1} = 3M_1$ and $L_{m2} = 1.5M_2$, index l stands for leakage inductances, and $L_{s1}, L_{s2}, L_{r1}, L_{r2}$ are stator and rotor self-inductances.

$$\begin{aligned}
T_{e1} &= -P_1 M_1\\
&\quad \times\left\{\begin{array}{l}
(i_A i_{ar1} + i_B i_{br1} + i_C i_{cr1} + i_D i_{dr1} + i_E i_{er1} + i_F i_{fr1})\sin\theta_1\\
+(i_F i_{ar1} + i_A i_{br1} + i_B i_{cr1} + i_C i_{dr1} + i_D i_{er1} + i_E i_{fr1})\sin(\theta_1 - 5\alpha)\\
+(i_E i_{ar1} + i_F i_{br1} + i_A i_{cr1} + i_B i_{dr1} + i_C i_{er1} + i_D i_{fr1})\sin(\theta_1 - 4\alpha)\\
+(i_D i_{ar1} + i_E i_{br1} + i_F i_{cr1} + i_A i_{dr1} + i_B i_{er1} + i_C i_{fr1})\sin(\theta_1 - 3\alpha)\\
+(i_C i_{ar1} + i_D i_{br1} + i_E i_{cr1} + i_F i_{dr1} + i_A i_{er1} + i_B i_{fr1})\sin(\theta_1 - 2\alpha)\\
+(i_B i_{ar1} + i_C i_{br1} + i_D i_{cr1} + i_E i_{dr1} + i_F i_{er1} + i_A i_{fr1})\sin(\theta_1 - \alpha)
\end{array}\right\}
\end{aligned} \tag{9}$$

$$\begin{aligned}
T_{e2} &= -P_2 M_2\\
&\quad \times\left\{\begin{array}{l}
((i_A + i_D)i_{ar2} + (i_B + i_E)i_{br2} + (i_C + i_F)i_{cr2})\sin\theta_2\\
+((i_C + i_F)i_{ar2} + (i_A + i_D)i_{br2} + (i_B + i_E)i_{cr2})\sin(\theta_2 - 4\alpha)\\
+((i_B + i_E)i_{ar2} + (i_C + i_F)i_{br2} + (i_A + i_D)i_{cr2})\sin(\theta_2 - 2\alpha)
\end{array}\right\}
\end{aligned} \tag{10}$$

$$\underline{C}_{(6)} = \sqrt{\frac{2}{6}}\begin{array}{c}\alpha\\ \beta\\ x\\ y\\ 0+\\ 0-\end{array}\left|\left[\begin{array}{cccccc}
1 & \cos\alpha & \cos 2\alpha & \cos 3\alpha & \cos 4\alpha & \cos 5\alpha\\
0 & \sin\alpha & \sin 2\alpha & \sin 3\alpha & \sin 4\alpha & \sin 5\alpha\\
1 & \cos 2\alpha & \cos 4\alpha & \cos 6\alpha & \cos 8\alpha & \cos 10\alpha\\
0 & \sin 2\alpha & \sin 4\alpha & \sin 6\alpha & \sin 8\alpha & \sin 10\alpha\\
1/\sqrt{2} & 1/\sqrt{2} & 1/\sqrt{2} & 1/\sqrt{2} & 1/\sqrt{2} & 1/\sqrt{2}\\
1/\sqrt{2} & -1/\sqrt{2} & 1/\sqrt{2} & -1/\sqrt{2} & 1/\sqrt{2} & -1/\sqrt{2}
\end{array}\right]\right. \tag{11}$$

Application of the decoupling transformation on the torque equations (9) and (10) yields

$$T_{e1} = P_1 L_{m1} \begin{bmatrix} \cos\theta_1 \left(i_{\alpha r1} i_\beta^{\mathrm{INV}} - i_{\beta r1} i_\alpha^{\mathrm{INV}}\right) \\ -\sin\theta_1 \left(i_{\alpha r1} i_\alpha^{\mathrm{INV}} + i_{\beta r1} i_\beta^{\mathrm{INV}}\right) \end{bmatrix}$$
$$T_{e2} = P_2 L_{m2} \sqrt{2} \begin{bmatrix} \cos\theta_2 \left(i_{\alpha r2} i_y^{\mathrm{INV}} - i_{\beta r2} i_x^{\mathrm{INV}}\right) \\ -\sin\theta_2 \left(i_{\alpha r2} i_x^{\mathrm{INV}} + i_{\beta r2} i_y^{\mathrm{INV}}\right) \end{bmatrix}. \tag{16}$$

According to (15) and (16), flux/torque-producing stator currents of the six-phase machine are the inverter α–β current components, while the flux/torque-producing stator currents of the three-phase machine are the inverter x–y current components. This indicates the possibility of independent vector control of two machines, as predicted in [6]. Inverter voltage equations (15) can be given in terms of axis voltage components of the two machines as

$$\begin{bmatrix} v_\alpha^{\mathrm{INV}} \\ v_\beta^{\mathrm{INV}} \\ v_x^{\mathrm{INV}} \\ v_y^{\mathrm{INV}} \\ v_{0+}^{\mathrm{INV}} \\ v_{0-}^{\mathrm{INV}} \end{bmatrix} = \underline{C}_{(6)} \begin{bmatrix} v_{as1} + v_{as2} \\ v_{bs1} + v_{bs2} \\ v_{cs1} + v_{cs2} \\ v_{ds1} + v_{as2} \\ v_{es1} + v_{bs2} \\ v_{fs1} + v_{cs2} \end{bmatrix} = \begin{bmatrix} v_{\alpha s1} \\ v_{\beta s1} \\ v_{xs1} + \sqrt{2} v_{\alpha s2} \\ v_{ys1} + \sqrt{2} v_{\beta s2} \\ v_{0+s1} + \sqrt{2} v_{0s2} \\ v_{0-s1} \end{bmatrix}. \tag{17}$$

Similarly, individual flux/torque-producing currents of the two machines are related with the inverter current axis components by

$$\begin{aligned} i_\alpha^{\mathrm{INV}} &= i_{\alpha s1} \qquad i_\beta^{\mathrm{INV}} = i_{\beta s1} \\ i_x^{\mathrm{INV}} &= i_{xs1} = i_{\alpha s2}/\sqrt{2} \qquad i_y^{\mathrm{INV}} = i_{ys1} = i_{\beta s2}/\sqrt{2} \\ i_{0+}^{\mathrm{INV}} &= i_{0+s1} = i_{0s2}/\sqrt{2} \qquad i_{0-}^{\mathrm{INV}} = i_{0-s1}. \end{aligned} \tag{18}$$

C. Model in the Stationary Common Reference Frame

The rotational transformation, leading to the d-q system of equations, is applied next in conjunction with the rotor equations. The matrix for the six-phase machine is given with

$$\underline{D}_{r1} = \begin{bmatrix} \cos\theta_1 & -\sin\theta_1 & \\ \sin\theta_1 & \cos\theta_1 & \\ & & [\underline{I}]^{4\times 4} \end{bmatrix} \tag{19}$$

where $\underline{I}$ is the diagonal 4×4 unity matrix. The transformation matrix for the three-phase machine is of the same form, except that the rotor angular position is θ_2 and the matrix dimensions are 3×3.

Since, according to (13) and (14), rotor equations for x–y and zero-sequence components are completely decoupled from the rest of the system and these circuits cannot be excited, these equations can be omitted from further consideration. Upon application of the rotational transformation the voltage equations for the two rotor windings in the stationary common reference frame become

$$\begin{aligned} 0 &= R_{r1} i_{dr1} + L_{m1} \frac{di_d^{\mathrm{INV}}}{dt} + L_{r1} \frac{di_{dr1}}{dt} \\ &\quad + \omega_1 \left(L_{m1} i_q^{\mathrm{INV}} + L_{r1} i_{qr1}\right) \\ 0 &= R_{r1} i_{qr1} + L_{m1} \frac{di_q^{\mathrm{INV}}}{dt} + L_{r1} \frac{di_{qr1}}{dt} \\ &\quad - \omega_1 \left(L_{m1} i_d^{\mathrm{INV}} + L_{r1} i_{dr1}\right) \end{aligned} \tag{20}$$

$$\begin{aligned} 0 &= R_{r2} i_{dr2} + \sqrt{2} L_{m2} \frac{di_x^{\mathrm{INV}}}{dt} + L_{r2} \frac{di_{dr2}}{dt} \\ &\quad + \omega_2 \left(L_{m2} \sqrt{2} i_y^{\mathrm{INV}} + L_{r2} i_{qr2}\right) \\ 0 &= R_{r2} i_{qr2} + \sqrt{2} L_{m2} \frac{di_y^{\mathrm{INV}}}{dt} + L_{r2} \frac{di_{qr2}}{dt} \\ &\quad - \omega_2 \left(L_{m2} \sqrt{2} i_x^{\mathrm{INV}} + L_{r2} i_{dr2}\right) \end{aligned} \tag{21}$$

while the source equations are given with

$$\begin{aligned} v_d^{\mathrm{INV}} &= R_{s1}\, i_d^{\mathrm{INV}} + L_{s1} di_d^{\mathrm{INV}} \big/ dt + L_{m1} di_{dr1}/dt \\ v_q^{\mathrm{INV}} &= R_{s1}\, i_q^{\mathrm{INV}} + L_{s1} di_q^{\mathrm{INV}} \big/ dt + L_{m1} di_{qr1}/dt \\ v_x^{\mathrm{INV}} &= R_{s1}\, i_x^{\mathrm{INV}} + L_{ls1} di_x^{\mathrm{INV}} \big/ dt + \sqrt{2} \Big\{ R_{s2} \sqrt{2} i_x^{\mathrm{INV}} \\ &\qquad + L_{s2} d\sqrt{2} i_x^{\mathrm{INV}} \Big/ dt + L_{m2} di_{dr2}/dt \Big\} \\ v_y^{\mathrm{INV}} &= R_{s1}\, i_y^{\mathrm{INV}} + L_{ls1} di_y^{\mathrm{INV}} \big/ dt + \sqrt{2} \Big\{ R_{s2} \sqrt{2} i_y^{\mathrm{INV}} \\ &\qquad + L_{s2} d\sqrt{2} i_y^{\mathrm{INV}} \Big/ dt + L_{m2} di_{qr2}/dt \Big\} \\ v_{0+}^{\mathrm{INV}} &= R_{s1}\, i_{0+}^{\mathrm{INV}} + L_{ls1} di_{0+}^{\mathrm{INV}} \big/ dt \\ &\qquad + \sqrt{2} \Big\{ R_{s2} \sqrt{2}\, i_{0+}^{\mathrm{INV}} + L_{ls2} d\sqrt{2} i_{0+}^{\mathrm{INV}} \Big/ dt \Big\} \\ v_{0-}^{\mathrm{INV}} &= R_{s1}\, i_{0-}^{\mathrm{INV}} + L_{ls1} di_{0-}^{\mathrm{INV}} \big/ dt. \end{aligned} \tag{22}$$

Torque equations (16) become

$$\begin{aligned} T_{e1} &= P_1 L_{m1} \left[i_{dr1} i_q^{\mathrm{INV}} - i_d^{\mathrm{INV}} i_{qr1} \right] \\ T_{e2} &= \sqrt{2} P_2 L_{m2} \left[i_{dr2} i_y^{\mathrm{INV}} - i_x^{\mathrm{INV}} i_{qr2} \right]. \end{aligned} \tag{23}$$

Equations (17) and (18) remain to be valid in an unchanged form, with the replacement of indexes α, β with d, q.

Model (20)–(23) in the stationary reference frame shows that the rotor of the six-phase machine is coupled only with inverter d-q currents, while rotor of the three-phase machine couples with inverter x–y currents. Consequently, inverter d–q currents govern the torque production of the six-phase machine, while torque production of the three-phase machine is determined with inverter x–y currents. It therefore follows that the specific connection of the stator windings, shown in Fig. 1, can enable independent dynamic control of the two series-connected machines, using vector control principles.

D. Model in Rotor-Flux-Oriented Reference Frames

The simplest way to proceed further is to take the equations in the stationary reference frame (20)–(22) and define the following space vectors:

$$\underline{v}_{dq}^{\rm INV} = v_d^{\rm INV} + jv_q^{\rm INV} \qquad \underline{i}_{dq}^{\rm INV} = i_d^{\rm INV} + ji_q^{\rm INV}$$
$$\underline{v}_{xy}^{\rm INV} = v_x^{\rm INV} + jv_y^{\rm INV} \qquad \underline{i}_{xy}^{\rm INV} = i_x^{\rm INV} + ji_y^{\rm INV}$$
$$\underline{i}_{r1} = i_{dr1} + ji_{qr1} \qquad \underline{i}_{r2} = i_{dr2} + ji_{qr2}. \tag{24}$$

The first four equations of (22) can then be written in compact form as

$$\underline{v}_{dq}^{\rm INV} = R_{s1}\,\underline{i}_{dq}^{\rm INV} + L_{s1} d\underline{i}_{dq}^{\rm INV}\big/ dt + L_{m1} d\underline{i}_{r1}/dt$$
$$\underline{v}_{xy}^{\rm INV} = R_{s1}\,\underline{i}_{xy}^{\rm INV} + L_{ls1} d\underline{i}_{xy}^{\rm INV}\big/ dt + \sqrt{2} \cdot \left\{ R_{s2}\sqrt{2}\underline{i}_{xy}^{\rm INV} + L_{s2} d\sqrt{2}\underline{i}_{xy}^{\rm INV}\Big/ dt + L_{m2} d\underline{i}_{r2}/dt \right\}. \tag{25}$$

Transformation is done next separately for the inverter d–q equations and rotor equations of the six-phase machine, and the inverter x–y equations and rotor equations of the three-phase machine. This is possible since there exists full decoupling between the inverter d–q and x-y currents. Rotor-flux-oriented reference frames are defined with the angle of transformation and angular speed using $\phi_{r1} = \int \omega_{r1}\, dt$ and $\phi_{r2} = \int \omega_{r2}\, dt$ for the two machines, respectively. Correlation between current and voltage space vectors in the stationary and in the rotor-flux-oriented reference frames is given with

$$\underline{f}_{dq}^{(1)} = \underline{f}_{dq} \exp(j\phi_{r1})$$
$$\underline{f}_{xy}^{(2)} = \underline{f}_{xy} \exp(j\phi_{r2}). \tag{26}$$

Application of (26) in conjunction with the model in the stationary reference frame (20)–(22) yields the equations in the rotor-flux-oriented reference frames. Inverter d-q equations and rotor equations of the six-phase machine are expressed in the reference frame fixed to the rotor flux of the six-phase machine [additional superscript (1)]. Similarly, inverter x–y voltage equations and rotor equations of the three-phase machine are given in the reference frame attached to the rotor flux of the three-phase machine [additional superscript (2)]. The zero-sequence equations remain the same as in (22) and are, therefore, not repeated. The final model is given with

$$\underline{v}_{dq}^{INV(1)} = R_{s1}\,\underline{i}_{dq}^{INV(1)} + L_{s1} d\underline{i}_{dq}^{INV(1)}\Big/ dt + L_{m1}\, d\underline{i}_{r1}^{(1)}\Big/ dt + j\omega_{r1}\left[L_{s1}\underline{i}_{dq}^{INV(1)} + L_{m1}\underline{i}_{r1}^{(1)}\right]$$
$$\underline{v}_{xy}^{INV(2)} = (R_{s1} + 2R_{s2})\underline{i}_{xy}^{INV(2)} + (L_{ls1} + 2L_{s2})\, d\underline{i}_{xy}^{INV(2)}\Big/ dt + L_{m2}\sqrt{2}\, d\underline{i}_{r2}^{(2)}\Big/ dt + j\omega_{r2}\left[(L_{ls1} + 2L_{s2})\underline{i}_{xy}^{INV(2)} + \sqrt{2}L_{m2}\underline{i}_{r2}^{(2)}\right] \tag{27}$$

$$0 = R_{r1}\underline{i}_{r1}^{(1)} + L_{m1}\, d\underline{i}_{dq}^{INV(1)}\Big/ dt + L_{r1}\, d\underline{i}_{r1}^{(1)}\Big/ dt + j(\omega_{r1} - \omega_1)\left(L_{m1}\underline{i}_{dq}^{INV(1)} + L_{r1}\underline{i}_{r1}^{(1)}\right) \tag{28}$$

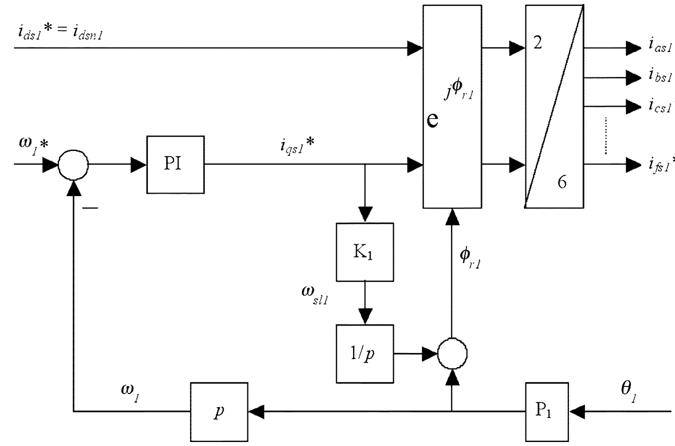

Fig. 2. Indirect (feedforward) rotor-flux-oriented controller for the six-phase induction machine $(K_1 = 1/(T_{r1}^* i_{ds1}^*), p \equiv d/dt)$.

$$0 = R_{r2}\underline{i}_{r2}^{(2)} + \sqrt{2}L_{m2}\, d\underline{i}_{xy}^{INV(2)}\Big/ dt + L_{r2}\, d\underline{i}_{r2}^{(2)}\Big/ dt + j(\omega_{r2} - \omega_2)\left(L_{m2}\sqrt{2}\underline{i}_{xy}^{INV(2)} + L_{r2}\underline{i}_{r2}^{(2)}\right). \tag{29}$$

Torque equations of the two machines (23) essentially do not change the form

$$T_{e1} = P_1 L_{m1}\left[i_{dr1}^{(1)} i_q^{INV(1)} - i_d^{INV(1)} i_{qr1}^{(1)}\right]$$
$$T_{e2} = \sqrt{2}P_2 L_{m2}\left[i_{dr2}^{(2)} i_y^{INV(2)} - i_x^{INV(2)} i_{qr2}^{(2)}\right]. \tag{30}$$

IV. Vector Control of the Two-Motor Drive

As the model (27)–(30) indicates, the two series-connected machines can be controlled independently using rotor-flux-oriented control principles. Flux and torque of the six-phase machine are controllable by inverter d-q-axis current components, while flux and torque of the three-phase machine can be controlled using inverter x–y current components. Indirect (feedforward) rotor-flux-oriented control is considered and current control in the stationary reference frame is assumed and exercised upon the inverter phase currents. The vector controller is of the same structure for both machines and is illustrated for the six-phase machine in Fig. 2. Individual phase current references of the two machines are given with $(k_1 = \sqrt{2/6}, k_2 = \sqrt{2/3})$

$$i_{as1}^* = k_1[i_{ds1}^* \cos\phi_{r1} - i_{qs1}^* \sin\phi_{r1}]$$
$$i_{bs1}^* = k_1[i_{ds1}^* \cos(\phi_{r1} - \alpha) - i_{qs1}^* \sin(\phi_{r1} - \alpha)]$$
$$i_{cs1}^* = k_1[i_{ds1}^* \cos(\phi_{r1} - 2\alpha) - i_{qs1}^* \sin(\phi_{r1} - 2\alpha)]$$
$$i_{ds1}^* = k_1[i_{ds1}^* \cos(\phi_{r1} - 3\alpha) - i_{qs1}^* \sin(\phi_{r1} - 3\alpha)]$$
$$i_{es1}^* = k_1[i_{ds1}^* \cos(\phi_{r1} - 4\alpha) - i_{qs1}^* \sin(\phi_{r1} - 4\alpha)]$$
$$i_{fs1}^* = k_1[i_{ds1}^* \cos(\phi_{r1} - 5\alpha) - i_{qs1}^* \sin(\phi_{r1} - 5\alpha)] \tag{31a}$$

$$i_{as2}^* = k_2[i_{ds2}^* \cos\phi_{r2} - i_{qs2}^* \sin\phi_{r2}]$$
$$i_{bs2}^* = k_2[i_{ds2}^* \cos(\phi_{r2} - 2\alpha) - i_{qs2}^* \sin(\phi_{r2} - 2\alpha)]$$
$$i_{cs2}^* = k_2[i_{ds2}^* \cos(\phi_{r2} - 4\alpha) - i_{qs2}^* \sin(\phi_{r2} - 4\alpha)]. \tag{31b}$$

Phase current references for the two machines need further to be summed in order to create overall inverter phase current ref-

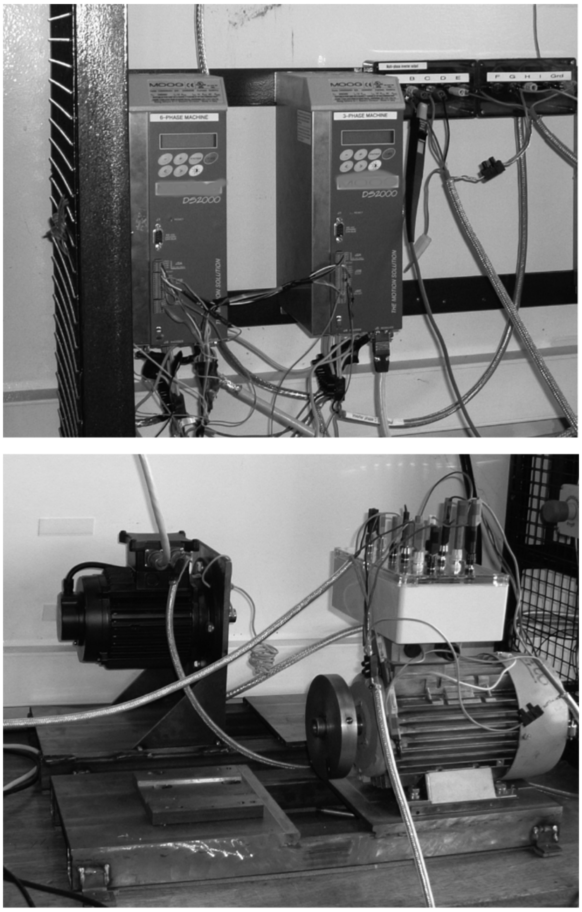

Fig. 3. Experimental rig: the six-phase voltage-source inverter and the six-phase (front) and three-phase (back) machine.

erences. Since each phase of the three-phase machine is connected to two phases of the six-phase machine, each inverter phase current reference has to consist of the sum of the six-phase machine phase current reference and one-half of the three-phase machine current reference. The inverter phase current references are, hence, created with the aid of the connection diagram of Fig. 1 in the following manner:

$$\begin{aligned} i_A^* &= i_{as1}^* + 0.5 i_{as2}^* & i_D^* &= i_{ds1}^* + 0.5 i_{as2}^* \\ i_B^* &= i_{bs1}^* + 0.5 i_{bs2}^* & i_E^* &= i_{es1}^* + 0.5 i_{bs2}^* \\ i_C^* &= i_{cs1}^* + 0.5 i_{cs2}^* & i_F^* &= i_{fs1}^* + 0.5 i_{cs2}^*. \end{aligned} \tag{32}$$

V. Experimental Setup

The experimental rig, illustrated in Fig. 3, utilizes two three-phase inverters with the common dc link, each of which is equipped with a digital signal processor (DSP). The inverters are rated at 14/42 A/A (continuous rms/peak). Each of them is equipped with a Texas Instruments TMS320F240 DSP. The first three-phase inverter supplies phases A, C, and E, while the second inverter supplies phases B, D, and F. All six currents are measured using LEM sensors. The current control rate and the inverter switching frequency are 10 kHz. PWM ripple is filtered out in the DSPs using finite-impulse response (FIR) filters, which average 2^n equidistant samples taken during one switching period. The current signal, which is now PWM-ripple-free, is further used as the input of the current controllers. The inverter DSPs perform closed-loop current control in the stationary reference frame using the ramp-comparison method in the most basic form [9] (hence, the problem of deviation of the actual motor phase current with respect to its reference will be experienced at higher operating frequencies [9]; this could be removed by employing improved current regulators [10], however, such a modification of the current controllers is beyond the scope of this paper). The inverter current references are passed to the DSPs from a PC, through a dedicated interface card. The control code is written in C. It performs closed-loop speed control and indirect rotor-flux-oriented control according to Fig. 2, in parallel for the two machines. Phase current references are calculated for the two machines using (31) and inverter phase current references are finally generated by means of (32).

The six-phase induction machine is obtained by rewinding the stator of a three-phase machine and is 50 Hz, six-pole. Rated phase-to-neutral voltage is 110 V and other relevant ratings are 1.1 kW, 2.7 A, and 900 r/min. The three-phase induction machine is an industrial servo-drive (1 kW, 120 Hz, four-pole, 325 V line-to-line). Both machines are equipped with resolvers and control operates in the speed-sensored mode. Closed-loop speed control is analyzed in experiments.

Various experimental tests are performed in order to verify the independence of the control of the two machines. The results are reported in the following section. Operation in the base speed region only is considered and the stator d-axis current references of both machines are constant at all times (1.5 A rms for each machine). Both machines are running under no-load conditions (except for the load torque application/removal transients).

VI. Experimental Results

The following approach is adopted in testing, with the idea of proving the decoupling of control of the two machines. Both machines are initially brought to a certain steady-state speed. A speed transient is initiated next for either the six-phase or the three-phase machine, while the operating speed of the other machine remains unchanged. Full decoupling of control will exist if and only if the speed and, more importantly, stator q-axis current command of the machine whose speed reference has not been altered do not change. The transients examined in experiments are acceleration, deceleration, reversing (which all take place under no-load conditions), and step loading/unloading transients.

In the first test the six-phase machine runs at 500 r/min (25 Hz) in the reverse direction, while the speed reference of the three-phase machine is initially 0 r/min. The speed reference of the three-phase machine is at $t = 0.2$ s stepped to 300 r/min (10 Hz). Fig. 4 illustrates speed responses and stator q-axis current references of the two machines. The corresponding phase current references of the two machines are shown in Fig. 5(a). Fig. 5(b) shows a comparison between inverter current reference created using (32) and the actual inverter phase current. It can be seen in Fig. 4 that initiation of a speed transient for the three-phase machine has no impact on the behavior of the six-phase machine since neither the speed nor the stator q-axis

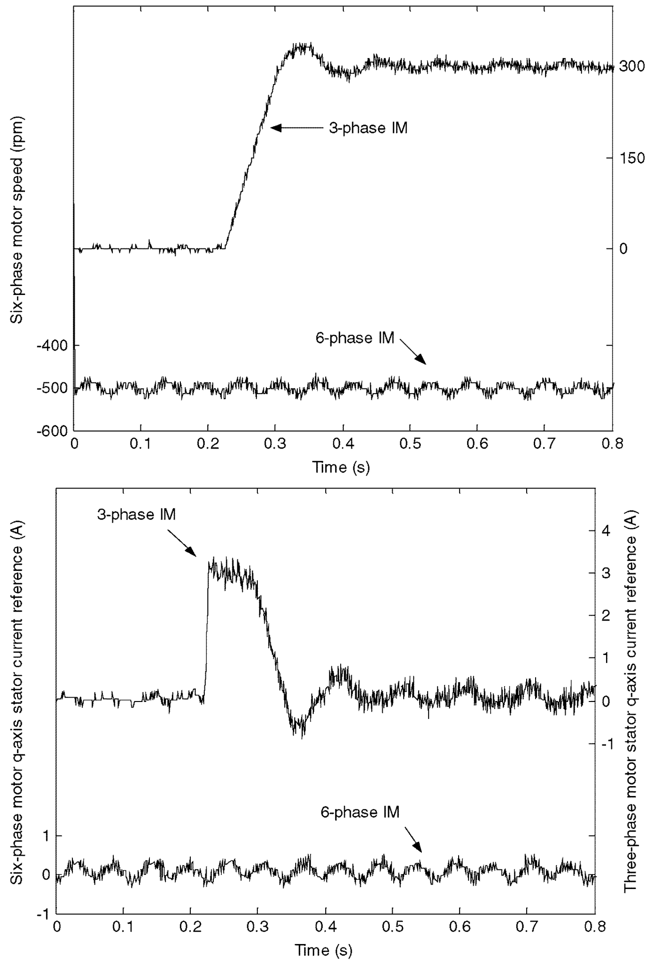

Fig. 4. Speed responses and stator q-axis current commands for an acceleration transient: six-phase machine runs at -500 r/min, while the three-phase machine is accelerated from 0 to 300 r/min.

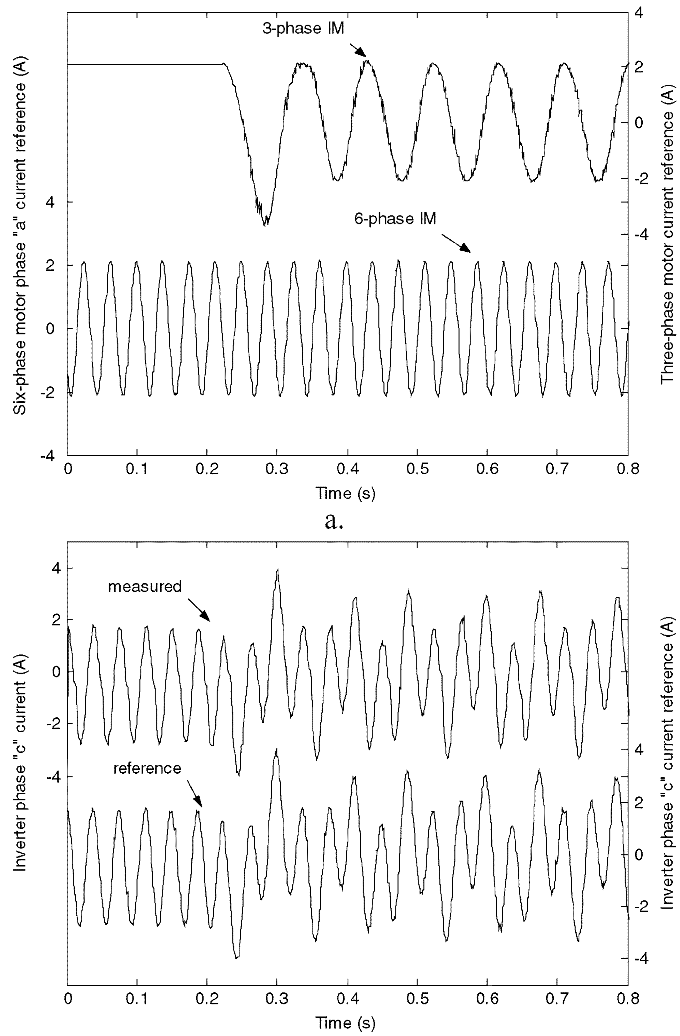

Fig. 5. (a) Stator phase current references for the two machines. (b) Comparison of measured and reference inverter phase current. Conditions of Fig. 4 apply.

current reference change. This is further confirmed by inspection of the phase current reference in Fig. 5(a) for the six-phase machine, which does not exhibit any change whatsoever during the transient of the three-phase machine. The inverter current [Fig. 5(b)] is in the previous steady state a sinusoidal function of approximately 25-Hz frequency with a dc offset caused by the stator d-axis current (magnetizing current) of the three-phase machine (which is at standstill). Upon completion of the transient, the inverter current is a sum of two sinusoidal functions of (31) with different frequencies and magnitudes that are obtained using (32). As can be seen from Fig. 5(b), measured and reference inverter current are in very good agreement.

In the second test, the role of the two machines is reversed, meaning that the transient is initiated for the six-phase machine. Deceleration is considered this time. The three-phase machine runs at constant 600-r/min (20 Hz) speed, while the six-phase machine is decelerated from an initial -800 r/min (40 Hz) to zero speed. Speed responses and stator q-axis current references for this transient are depicted in Fig. 6. It is evident from Fig. 6 that the speed of the three-phase machine remains unaffected by the transient of the six-phase machine. The same observation follows from traces of stator q-axis current references, where only a minor change in the ripple frequency (but not in magnitude) of the three-phase motor q-axis current reference can be observed. This is due to the change in the inverter noise characteristic that depends on the operating frequencies of both machines.

Some further reversing tests are conducted next to further verify decoupling of the control of the two machines. Fig. 7 displays results for the case when the speed of the three-phase machine is kept at zero, while the six-phase machine is reversed from -500 to 500 r/min. Both speed and stator q-axis current reference of the three-phase machine remain essentially unaffected by the reversing of the six-phase machine. The identical conclusion follows from Fig. 8 where the six-phase machine speed is kept at zero while the three-phase machine is reversed from 600 to -600 r/min. On this occasion, the six-phase machine is not affected by the transient of the three-phase machine as evidenced from the speed response and stator q-axis current reference of the six-phase machine. A comparison of measured and reference inverter current is included in both figures. These are, once more, in very good agreement.

A further test consists of the step load torque application on the three-phase machine, running at 1000 r/min. The six-phase machine runs at 400 r/min and the load torque applied to the

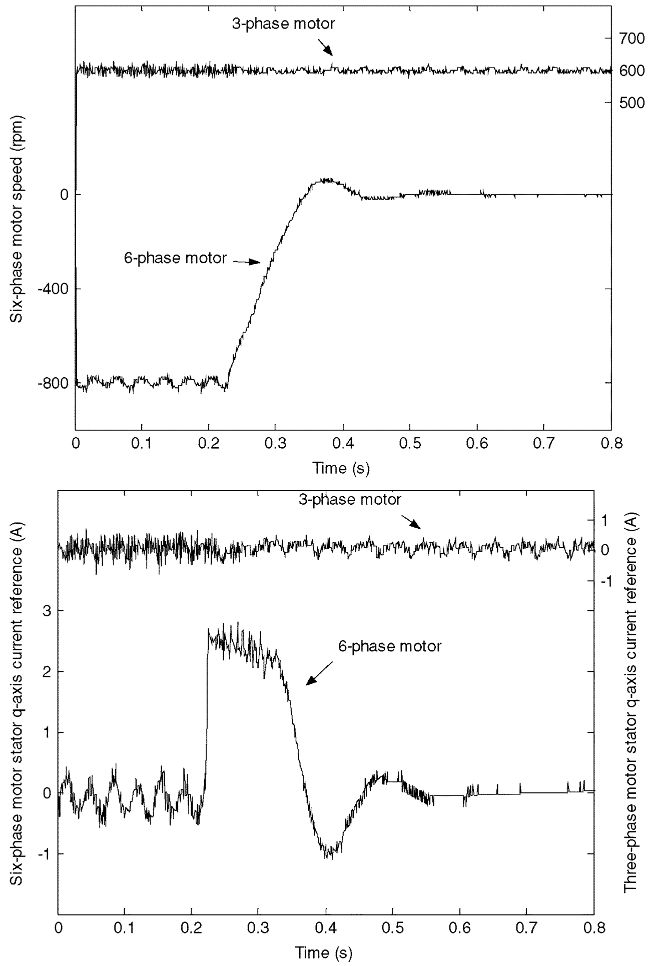

Fig. 6. Speed responses and stator q-axis current commands for a deceleration transient: three-phase machine runs at 600 r/min, while the six-phase machine is decelerated from -800 to 0 r/min.

three-phase machine is around 40%–45% of the rated torque. The speed responses and stator q-axis current references are shown in Fig. 9. No variation whatsoever can be observed in either the six-phase machine speed trace or the six-phase machine's q-axis current reference. Since the three-phase machine flux/torque-producing currents flow through the windings of the six-phase machine, this test, which asks for practically instantaneous change of the three-phase motor currents, can be taken as an ultimate proof of the truly independent control of the two machines.

The last test, illustrated in Fig. 10, is the step unloading of the six-phase machine at 500 r/min with the three-phase machine running at 800 r/min. In addition to the speed and stator q-axis current reference traces, measured and reference inverter currents, as well as current references for one phase of each machine, are included as well. It is evident from Fig. 10 that step unloading of the six-phase machine does not cause any disturbance in the three-phase machine's speed and stator q-axis current reference traces.

Some asymmetry is evident in the trace of the six-phase machine phase current reference (Fig. 10) before step unloading. This is the consequence of the stator q-axis current ripple. Although the ripple is practically the same in both no-load and loaded operation, its impact on the stator phase current peak

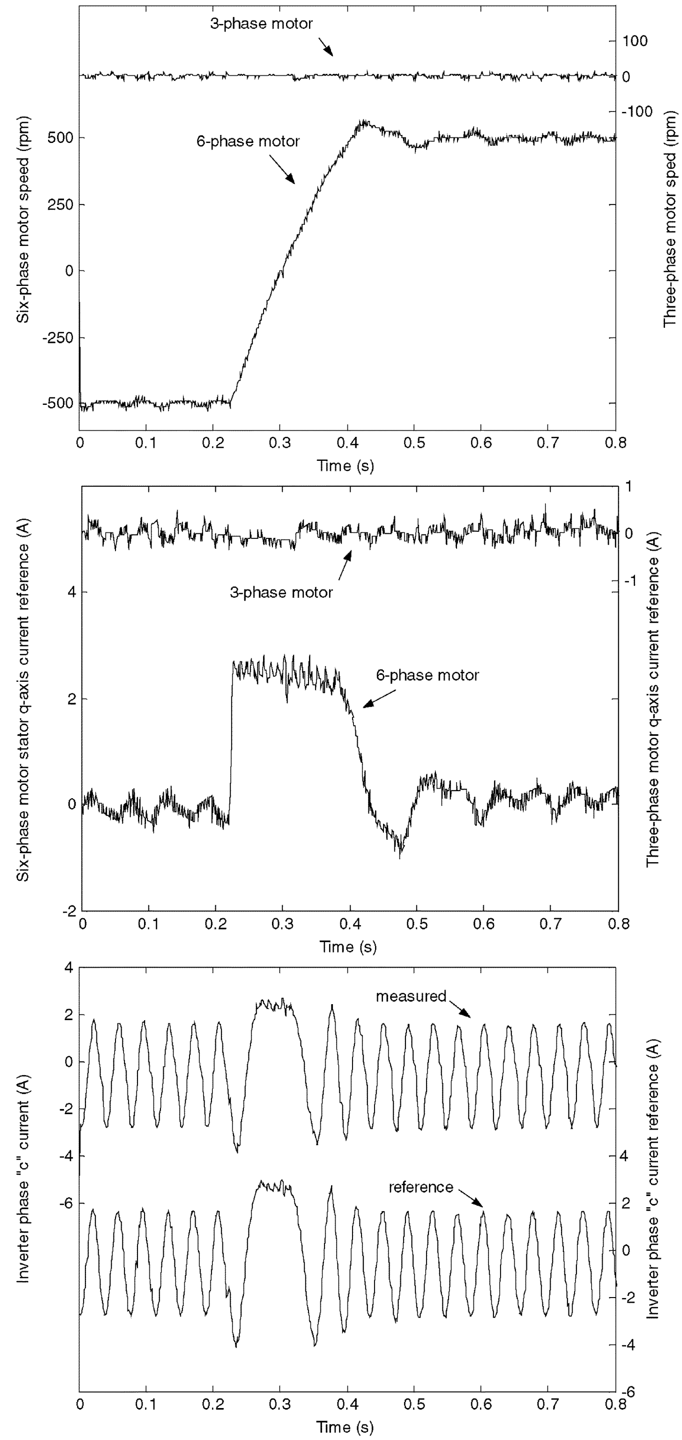

Fig. 7. Speed responses, stator q-axis current references, and a comparison between measured and reference inverter current for a reversing transient: three-phase machine at standstill, six-phase machine reversed from -500 to 500 r/min.

value increases with loading, due to an increase in the average stator q-axis current. Hence, the phase current reference exhibits some variation in the peak values, determined with the frequency of the ripple in the stator q-axis current.

It is felt that the origin of the torque (stator q-axis current) ripple in the six-phase machine deserves an explanation. Although transients of the three-phase machine do not cause a disturbance in the six-phase machine's torque (stator q-axis cur-

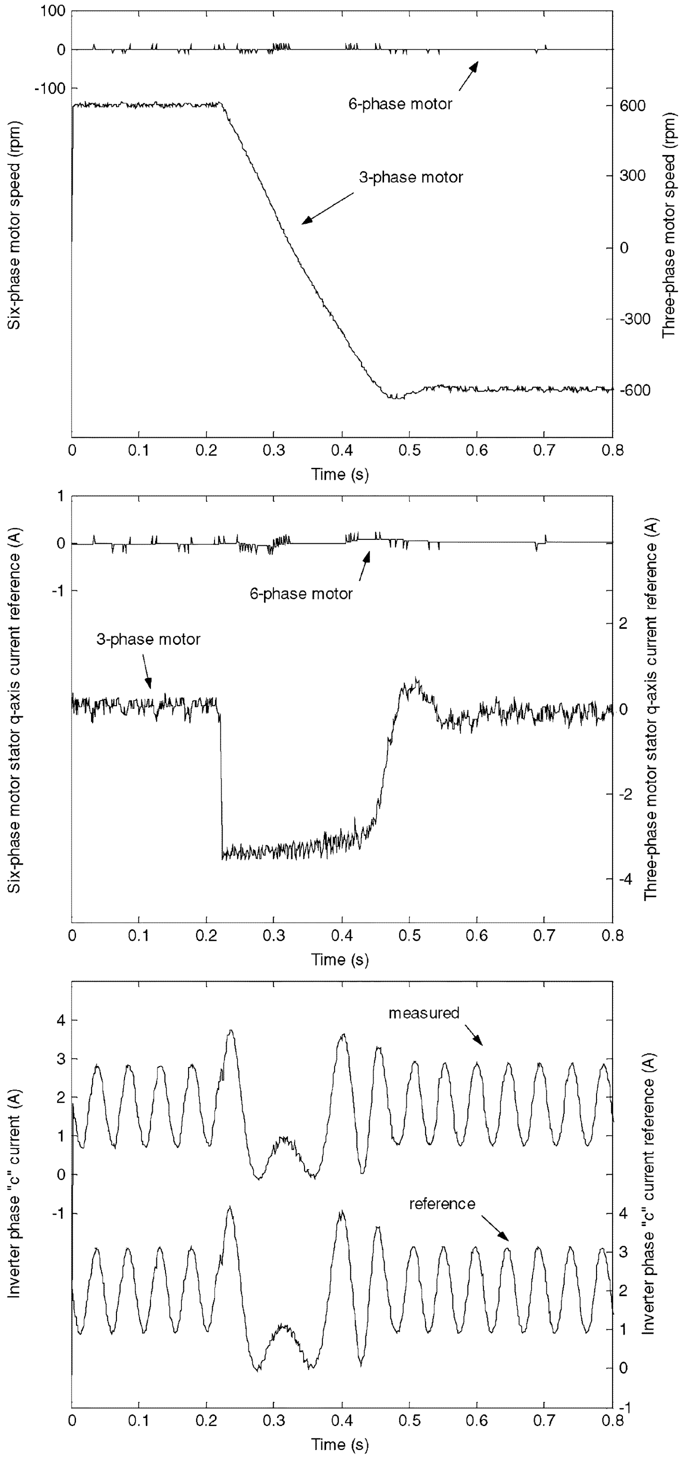

Fig. 8. Speed responses, stator q-axis current references, and a comparison between measured and reference inverter current for a reversing transient: six-phase machine at 0 r/min, three-phase machine 600 to -600 r/min.

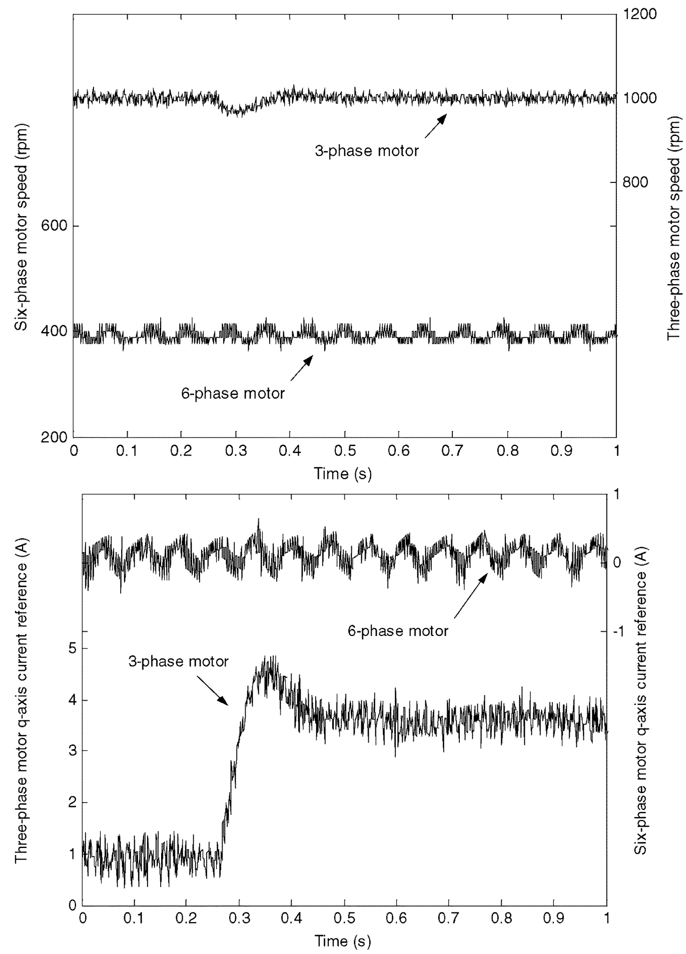

Fig. 9. Speed responses and stator q-axis current references during step loading of the three-phase motor running at 1000 r/min (six-phase machine runs at 400 r/min).

rent), the ripple at nonzero speeds (Figs. 4, 6, 7, 9, and 10) exceeds the amount that could be assigned to the measurement noise. However, the ripple is not caused by the series connection of the two machines, since it exists even when the six-phase machine is operated as a single vector-controlled drive (i.e., when the three-phase machine is disconnected). To prove this statement, Fig. 11 illustrates a speed reversal of the six-phase induction machine from -500 to 500 r/min (25 Hz). The three-phase machine has been removed from the setup for this experiment. The stator current spectrum in final steady state at 25 Hz is included as well. Torque ripple in Fig. 11 practically coincides with the ripple in Fig. 4 where the machine was running at -500 r/min. This confirms that the torque ripple is inherent to the six-phase machine. The stator current spectrum shows the presence of subharmonics at frequencies 1/3 (backward rotating field) and 5/3 (forward rotating field) of the fundamental frequency, which combine to yield a torque ripple with a frequency of 2/3 of the fundamental frequency under no-load conditions. On the basis of these considerations it is concluded that the torque ripple in the six-phase machine is caused by dynamic eccentricities of the second order.

VII. Conclusion

This paper has analyzed a six-phase series-connected two-motor drive system. The phase-variable model was initially introduced and the detailed modeling procedure was presented. The model is transformed using transformations of the general theory of electrical machines and the d–q-axis model in the stationary reference frame was developed. Properties of this model are such that they unambiguously show the possibility of decoupled vector control of the system, using

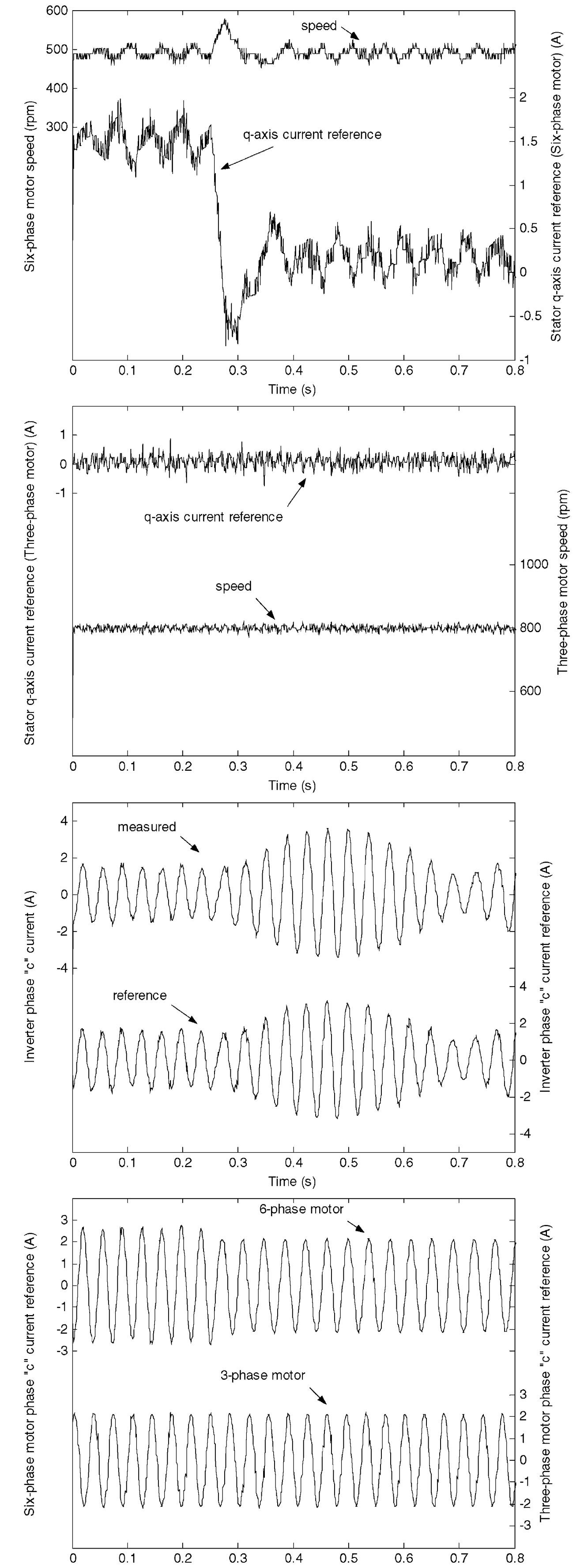

Fig. 10. Step unloading of the six-phase machine at 500 r/min with three-phase machine running at 800 r/min.

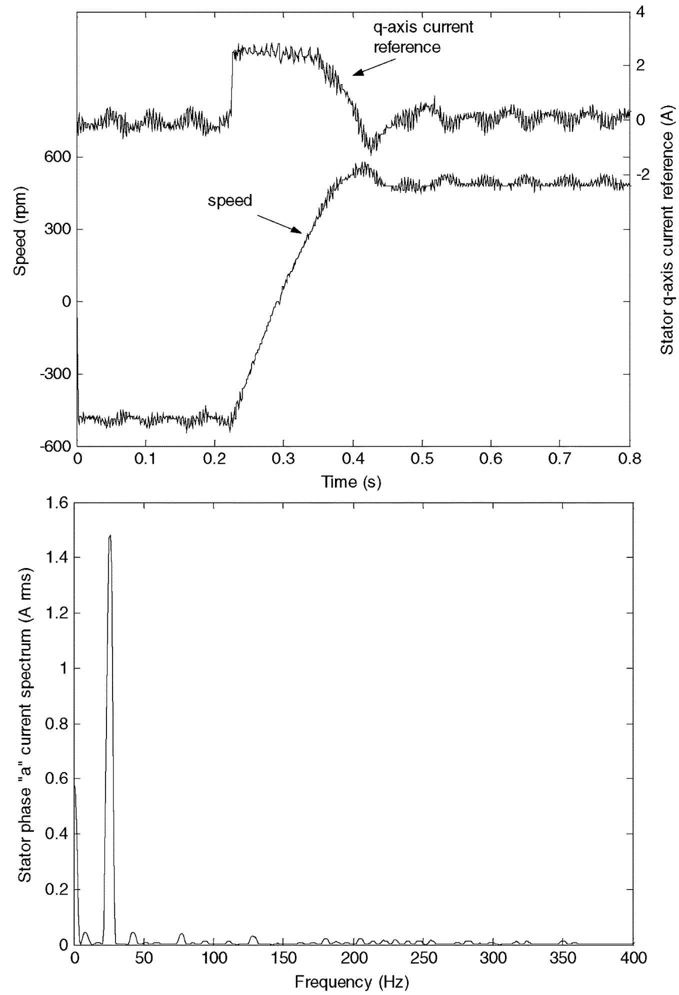

Fig. 11. Six-phase machine's speed reversal from −500 to 500 r/min and stator phase current spectrum at 500 r/min (25 Hz). The three-phase machine was disconnected in this experiment.

a single six-phase VSI. The model is finally transformed into rotor-flux-oriented reference frames of the two machines. On the basis of the resulting model, indirect vector control principles were developed for the two-motor structure that assume current control in the stationary reference frame.

An experimental rig was further described. This was followed by presentation of detailed experimental results for a number of transients. These include acceleration, deceleration, and reversing, as well as the loading transient. The results show that it is possible to independently operate two induction machines from a single inverter with completely decoupled control.

As already noted in Section I, the six-phase series-connected two-motor drive is well suited for applications where a six-phase motor drive is used anyway due to high power requirements. Since the six-phase inverter is then already in existence, the addition of the second machine does not require any new hardware. It is only necessary to slightly modify the software, which means that the investment in the control and supply of the second (three-phase) motor drive is practically nonexistent. This remark applies provided that the three-phase machine is of a reasonably low voltage rating, so that the inverter voltage margin is not jeopardized by the connection of the second machine. The three-phase machine has to be of a considerably smaller power rating than the six-phase machine, since the six-phase machine's stator winding losses increase due to the series connection with the three-phase machine (the three-phase machine is not adversely affected in any way by the series connection with the six-phase machine).

References

[1] R. H. Nelson and P. C. Krause, "Induction machine analysis for arbitrary displacement between multiple winding sets," *IEEE Trans. Power App. Syst.*, vol. PAS-93, no. 3, pp. 841–848, may/Jun. 1974.

[2] R. Bojoi, M. Lazzari, F. Profumo, and A. Tenconi, "Digital field oriented control for dual three-phase induction motor drives," in *Proc. IEEE-IAS Annu. Meeting*, Pittsburgh, PA, 2002, CD-ROM, Paper 22P1.

[3] D. Hadiouche, H. Razik, and A. Rezooug, "Design of novel winding configurations for VSI fed dual-stator induction machines," in *Proc. Electrimacs*, Montreal, QC, Canada, 2002, CD-ROM, Paper 263.

[4] R. Bojoi, A. Tenconi, F. Profumo, G. Griva, and D. Martinello, "Complete analysis and comparative study of digital modulation techniques for dual three-phase AC motor drives," in *Proc. IEEE PESC'02*, Cairns, Australia, 2002, CD-ROM, Paper 10159.

[5] R. O. C. Lyra and T. A. Lipo, "Torque density improvement in a six-phase induction motor with third harmonic current injection," *IEEE Trans. Ind. Applicat.*, vol. 38, no. 5, pp. 1351–1360, Sep./Oct. 2002.

[6] E. Levi, M. Jones, and S. N. Vukosavic, "Even-phase multi-motor vector controlled drive with single inverter supply and series connection of stator windings," *Proc. IEE—Elect. Power Appl.*, vol. 150, pp. 580–590, 2003.

[7] E. Levi, M. Jones, S. N. Vukosavic, and H. A. Toliyat, "A novel concept of a multiphase, multi-motor vector controlled drive system supplied from a single voltage source inverter," *IEEE Trans. Power Electron.*, vol. 19, no. 2, pp. 320–335, Mar. 2004.

[8] E. Levi, A. Iqbal, S. N. Vukosavic, and H. A. Toliyat, "Modeling and control of a five-phase series-connected two-motor drive," in *Proc. IEEE IECON'03*, Roanoke, VA, 2003, pp. 208–213.

[9] D. M. Brod and D. W. Novotny, "Current control of VSI-PWM inverters," *IEEE Trans. Ind. Appl.*, vol. IA-21, no. 4, pp. 562–570, Jul./Aug. 1985.

[10] T. M. Rowan and R. J. Kerkman, "A new synchronous current regulator and an analysis of current-regulated PWM inverters," *IEEE Trans. Ind. Appl.*, vol. IA-22, no. 4, pp. 678–690, Jul./Aug. 1986.

Martin Jones was born in Liverpool, U.K., in 1970. He received the B.Eng. degree (First Class Honors) and the Ph.D. degree from the Liverpool John Moores University, Liverpool, U.K., in 2001 and 2005, respectively.

In September 2001, he became a Research Student at the Liverpool John Moores University, where he is currently a Post-Doctoral Research Associate. His areas of research interest are vector control of ac machines and power electronics.

Dr. Jones was a recipient of the IEE Robinson Research Scholarship for his Ph.D. studies.

Slobodan N. Vukosavic (M'93) was born in Sarajevo, Bosnia, and Hercegovina, Yugoslavia, in 1962. He received the B.S., M.S., and Ph.D. degrees from the University of Belgrade, Belgrade, Yugoslavia, in 1985, 1987, and 1989, respectively.

He was with the Nikola Tesla Institute, Belgrade, Yugoslavia, until 1988, when he joined the ESCD Laboratory of Emerson Electric, St. Louis, MO. Since 1991, he has been the Project Leader at the Vickers Company, Milan, Italy. He currently holds the post of a Professor at the University of Belgrade. He has published extensively and has completed over 40 large R/D and industrial projects.

Emil Levi (S'89–M'92–SM'99) was born in Zrenjanin, Yugoslavia, in 1958. He received the Dipl.Ing. degree from the University of Novi Sad, Novi Sad, Yugoslavia, in 1982, and the M.Sc. and Ph.D. degrees from the University of Belgrade, Belgrade, Yugoslavia, in 1986 and 1990, respectively.

From 1982 to 1992, he was with the Department of Electrical Engineering, University of Novi Sad. In May 1992, he joined the Liverpool John Moores University, Liverpool, U.K., where, since September 2000, he has been a Professor of Electric Machines and Drives. He has published over 150 papers, including more than 40 in major journals.

Atif Iqbal was born in India in 1971. He received the B.Sc. and M.Sc. degrees from Aligarh Muslim University, Aligarh, India, in 1991 and 1996, respectively. He is currently working toward the Ph.D. degree at the Liverpool John Moores University, Liverpool, U.K.

He has been a Lecturer in the Department of Electrical Engineering, Aligarh Muslim University, since 1991. His principal research concerns induction motor drives.